Journal of Nuclear Research and Applications

Research Paper

DOI: 1024200/jon.2022.1018

Cited in: https://jonra.nstri.ir
Received: 26 September 2021, Accepted: 12 February 2022

Calculation of Gallium-68 Dose Factors for [^{68}Ga] DOTATATE Injected Patients: A Comparison with OLINDA Database

S. Karimkhani[1], H. Yousefnia[2]*, R. Faghihi[1], P. Gramifar[3], M. R. Parishan[1]

[1]*Department of Nuclear Engineering, School of Mechanical Engineering, Shiraz University, Shiraz, Iran*
[2]*Radiation Application Research School, Nuclear Science and Technology Research Institute (NSTRI), Tehran, P.O. Box: 14155-1339, Iran*
[3]*Research Center for Nuclear Medicine, Shariati Hospital, Tehran University of Medical Sciences, Tehran, Iran*

ABSTRACT

[68Ga] DOTATATE as a radiolabeled tracer is used for in vivo detection of neuroendocrine tumors in the PET/CT examinations. This study aims to calculate S-values in various organs in a voxelized-based Monte Carlo simulation approach for each patient individually. PET/CT images of 9 patients suspected of neuroendocrine cancer were acquired 60 minutes after injection of [68Ga] DOTATATE. After reshaping and registering CT images to the size of PET images, GATE/GEANT4 Monte Carlo (MC) toolkit was used with two inputs of CT images as voxelized attenuation map and PET images as a voxelized activity map for the calculation of the different organs dose. Voxelized dose maps were extracted in the target organs for different source organs. S-value volume histogram and absolute S-values based on the MIRD formalism were calculated. The highest S-values were observed for spleen, bladder, kidneys, liver, pituitary, and the lung with 6.26E-05 ± 1.47E-05, 5.17E-05 ± 3.08E-05, 3.41E-05 ± 7.68E-06, 2.08E-05 ± 4.12E-06, 1.62E-05 ± 5.74E-06 and 8.47E-06 ± 2.47E-06 mGy/MBq.S, respectively. The difference between the amounts of the calculated S-values and those presented in OLINDA software is mainly related to the anatomical difference of the patients with the standard phantom in OLINEDA software. This study showed that patient-specific dosimetry is necessary to calculate S-values.

***Keywords*:** Dose factors; [68Ga] DOTATATE; Neuroendocrine Tumors; Monte Carlo

I. Introductions

The neuroendocrine system consists of neurons, glands, and non-endocrine tissues, and the neurochemicals, hormones, and humoral signals they produce and receive, which generally regulate other organs' function in an integrated manner [1]. Neuroendocrine cells are peptide-producing cells that can develop into a wide range of neuroendocrine tumors (NETs), including gastrointestinal, bronchial, lung, pancreatic, and thymic NETs, as well as medullary thyroid cancer, paraganglioma, and pheochromocytoma [2]. Depending on the type, growth rate, and how they spread in different regions, these tumors create very different symptoms leading to diagnosis difficulties. Somatostatin is a polypeptide hormone that mediates its inhibitory effects through binding to the specific cell surface, G-protein–coupled receptors, of which five distinct subtypes (sst1–sst5) have been characterized [3, 4].

DOTATATE is absorbed on type 2 somatostatin receptors, and because this type of receptor increases at the surface of the neuroendocrine tumors, the [68Ga]DOTATATE can well detect

**Corresponding Author name:* H. Yousefnia
E-mail address: hyousefnia@aeoi.org.ir

this type of tumor. DOTA peptides can be labeled rapidly and effectively with (_^68)Gawhich means that the peptide mass used can be shallow [5]. The physical half-life 68Ga is in good agreement with the physiological half-life of the combined peptides. So, the development of (_^68)Ga radiolabeled drugs has been paralleled to peptide-based medications' growth over the past two decades [6]. (_^68)Ga is a positron emitter radionuclide with a high application in nuclear medicine, which has been widely used to detect malignancies, especially NETs. The significance of (_^68)Ga radionuclide has been increased as theranostic radionuclide binding with radionuclides used in targeted radiotherapy (TRT) such as (_^90)Y and (_^177)Lu, and a variety of (_^68)Ga-SST complexes have entered into clinical applications with interesting pharmacokinetic and pharmacodynamics [7, 8]. Typically, the most important (_^68)Ga peptide radiolabeled drugs are somatostatin analogs such as [68Ga]DOTA_TOC, [68Ga]DOTATATE, and [68Ga]DOTANOC used in clinical studies [9]. The pharmacokinetic, blood purification, and accumulation in the target are compatible with a half-life of 68Ga. Renal excretion, short scan time, high sensitivity, high resolution and high contrast, high-quality images of the organs, and relatively small radiation dose are among the advantages that considered these analogs [10, 11].

One of the most important factors to be considered in evaluating new radiopharmaceuticals used for treatment and diagnosis is the absorbed dose of radionuclide in the body. At present, patient-specific dosimetry (PSD), known as the most accurate method in internal dosimetry, is used to optimize treatment and diagnosis procedures in nuclear medicine [12]. The PSD calculates the proper radiation dose received to each of the patient's internal organs according to the actual activity distribution of the injected adiopharmaceuticals. It is vital to estimate the precise dose of the patient instead of a conservative prediction for many cancerous patients who can potentially carry out further scans [13].

A 3D PSD study using [(_^68)Ga]DOTATATE PET/CT scan is essential for improving the design and treatment [14]. Therefore, activity and attenuation maps are needed to determine the actual activity distribution inside the patient body as well as the location and size of the organs of the patient. Dose factors calculation can be considered as the first step for PSD. In recent years, many studies have been conducted in internal dosimetry. Generally, ready-made phantoms such as the XCAT phantom are used for dosimetry, a three-dimensional phantom for both males and females. However, in some cases, CT-based images can pinpoint the exact location of target and source organs with dimensions commensurate with the patient's weight and height. This method is a more accurate but time-consuming method that differs significantly from three-dimensional phantoms calculations. When calculations are based on XCAT phantom data instead of patient CT images, the results are not accurate due to the anatomical difference between the patients.

In the present study, gallium-68 dose factors for Iranian patients suspected of developing neuroendocrine cancer were calculated after injection of [(_^68)Ga]DOTATATE radiopharmaceuticals. While the determination of 68Ga S-value has not been reported in the literature, the S-values have been only calculated for some standard phantoms and presented in OLINDA/EXM version 1.0 or similar software. This study was aimed to calculate 68Ga S-values according to the images captured from a number of Iranian patients for the first time with respect to the specific dosimetry. It should be mentioned that continuing this work for more patients can lead to the determination of the S-values with higher accuracy for Iranian patients. Also, it can result in modeling an Iranian phantom for the dosimetry of patients under diagnosis or therapy with different adiopharmaceuticals.

For this purpose, the required patient's anatomical information and activity distribution inside the patient's body were obtained from hybrid imaging PET/CT. The Monte Carlo method was used to calculate the radiation transport inside patient’s bodies. S-values, which are used to calculate the received doses in different organs from [(_^68)Ga]DOTATATE distribution inside the

body were extracted for each patient and compared with dose factors of OLINDA software, as the most commonly used database for patient-internal dosimetry.

II. Materials and methods

Patients

Patients were scanned by PET/CT (Biograph 6 True X; Siemens Medical Solutions) in the Shariati Hospital in Tehran, Iran. According to the previous studies, about 5 mCi of [(_^68)Ga]DOTATATE was injected, and after 60 minutes, PET/CT images were taken from patients in approximately 40 minutes and 7 to 11 beds (the time taken for each bed was about 4 minutes). In this process, each region of the patient's body (about 13 centimeters) was scanned for 4 minutes based on photon counting statistics. Scattering and attenuation correction was done using CT data.

Figure 1 shows the PET/CT images of P3 and P4. This figure illustrates spatial activity distribution and the location of tumors. As Figure 1 shows, the locations of lesions in P4 are (1) cervical zone, (2) left supraclavicular, (3) occiput-parietal region of skull, (4) paraaortic at the level of the supramesenteric artery, (5) retrocrural region, and (6) esophagus. The two last images show four lesions in P3 located at (1) hepatic segment II, (2) hepatic segment VIII, (3) hepatic segment IVB/V, and (4) hepatic segment V. Information of patients is brought in Table 1.

Images Registration

While the PET images were in the matrix size of 168 × 168 × n (n is the number of slices), and voxel size of 4.073 × 4.073 × 3 mm^3, the CT images were in the matrix size of 512 × 512 × n, and voxel size of 1.37 × 1.37 × 3 mm^3. In the procedure of PSD calculations, PET and CT images are used as the radiopharmaceutical biodistribution and attenuation map as the input data to the Monte Carlo (MC) code. Before segmenting the organs, these images should be matched in terms of the matrix size and the voxel, so misalignment is eliminated. In this study, the running time was reduced so that the patient's dosimetry could be done in the shortest possible time. Image registration was done using 3D Slicer, an open-source software platform for medical image informatics, image processing, and three-dimensional visualization. To manage the run time of MC simulation, in the registration step, the matrix size of CT images set to 168 × 168 × n, and voxel size set to 4.073 × 4.073 × 3 mm^3 leading to a little degradation of the CT images quality (Figure 2 (a) and (b)).

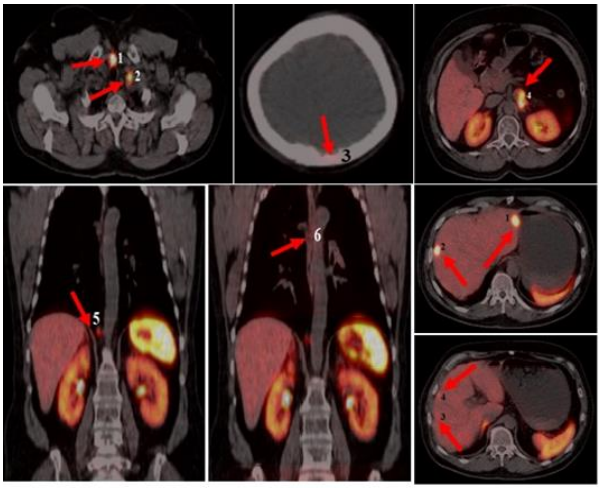

Figure 1. PET/CT images of p3 and p4. The patients were scanned 60 minutes after injection of about 5mCi of ^{68}Ga-DOTATATE. The five first images show the locations of six tumors of the p4 (tumor 3 and tumor 6 of this patient is not clear in these figures). The two last images show the locations of four tumors of the p3.

Table 1. The Patient characteristics.

patient	Gender	Age (y)	Weight (kg)	Height (cm)	Administered activity (MBq)	Tumor location (number)
P1	M	76	75	165	185.00	pancreatic(2), liver(2)
P2	F	73	45	145	159.10	-
P3	M	56	94	187	185.00	liver(4)
P4	F	56	82	170	185.00	cervical lymph nodes(2), skull(1), left adrenal gland(1), diaphragm lymph node(1), aortocaval lymph node(1)
P5	M	51	86	178	192.40	lesser curvature of gastric(1)
P6	F	51	84	170	179.45	pancreatic(1), cervical lymph nodes(1), left adrenal gland(1)
P7	F	42	64	174	185.00	-
P8	F	31	62	160	159.10	-
P9	F	16	56	159	185.00	-

Segmentation

The target organs are determined and segmented according to the differences in absorption of [^{68}Ga]DOTATATE in different organs and the location of the neuroendocrine tumor. To evaluate the effect of the total activity in the patient body on the dose of the target organs, the activity accumulated in the body was obtained from the PET images. Using unregistered CT images and 3D Slicer software, the internal organs were segmented and then registered as previously. Segmentation on unregistered images increases the accuracy of segmented organs. Figures 2 (c,d) show the segmented organs while the RadiAnt DICOM Viewer software fused PET and CT images. The part of the body below the thigh was cut away to decrease simulation run time. To prepare the input file of MC code, MATLAB software was used to assign a given code to each segmented organ and put them together to form a union attenuation map. Figures 2 (e and f) depict segmented organs as input files to Gate code. To obtain S-values individually for different organs, four organs of the spleen, kidneys, liver, and tumor were segmented from the PET images in the MATLAB. They were given to the MC code as voxelized sources. In order to use the attenuation and activity maps as the input data in the MC code, Xmedcon, was utilized. Xmedcon is an open-source medical image conversion toolkit that can change the data to Interfile format.

MC simulation

The GATE software needs input data as well as programming to simulate and calculate the required data. The GATE software requires two main inputs attenuation map and activity map. The attenuation map data were obtained from CT images, and PET images prepared the activity map data. In fact, the CT images were captured to visualize the body geometry of the patients, and the PET images were captured to determine organ activities. These data were processed using 3D Slicer and MATLAB software and used as the GATE software input data. The data was considered the interfile (with the suffixes of .i33 and .h33) and entered into the GATE software for further calculation.

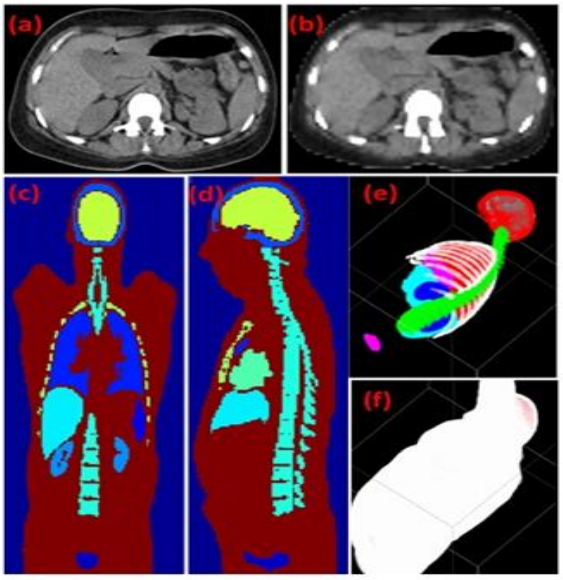

Figure 2. (a) The main CT image in the size of 512×512. (b) The reshaped and registered CT image to the size of the PET image. Clearly, the lower resolution and degradation of this image compared to the main image (a) is observable. (c) and (d) selectes mask of different organs, a patient in the segmentation step from two different views, each color shows a different organ. (e) The segmented organs are integrated together as one of the input files to the Gate/Geant 4. (f) The same as the (e), but the rest of the body, except of segmented organs, is assumed to be water, equal in the definition of materials in the Monte Carlo code simulation.

After importingthe raw data, including voxelized phantom and voxelized source, to the GATE/GEANT4 MC code, the physics model was set. The voxelized source consists of information about the activity range and PET images. At the same time, the voxalized phantom covers the data about the attenuation range and CT images. The activity range is different for each patient and was obtained according to the PET images. The activity range is a matrix gained according to the numerical value in each voxel of the PET images.

^{68}Ga was assumed as the isotopic pure positron emitter radionuclide with a spectrum of energy [15]. In this set of simulations, all physical interaction processes, including photoelectric absorption, Compton scattering, electron ionization, bremsstrahlung, electron and positron multiple scattering, and positron annihilation, were considered in the standard model. Also, the Rayleigh scattering process was set to the Penelope

model. The value of 100 eV was defined as the cut-off energy.

In this way, the effects of the emitted gamma rays and charged particles, except positrons, from the radionuclide are neglected, causing uncertainties in the deposited doses and final S-values, but effectively enhance the run time efficiency management procedures. Deposited doses in the various pre-segmented organs were extracted as output data. In order to investigate the effects of source simulation as a pure beta emitter, an ion source simulation was performed for the two patients considering all the energies associated with this radiopharmaceutical. The results did not make much difference, but the running time became longer. The simulation was carried out until the statistical error in several consecutive running was less than one percent.

Dose factor calculation

The MIRD formalism is a mathematical explanation of the transmitted energy from a source to a specific target. The most commonly used application of the MIRD formalism is in diagnostic nuclear medicine, which is generally used to estimate the risk of radiation effects and is equally appropriate for therapeutic purposes if the source and target volume can be determined accurately [16].

According to the MIRD formalism, the PSD is obtained individually from the biodistribution of activity in the patient body. PET images provide internal training at the voxel level. So, we can give the S-value according to the voxelized geometry of the PET image data set. The S-value of a given voxel is defined as the average absorbed dose in the target voxel in any radioactive decay in the source voxel.

In theory, S-value is calculated using the following equation, and its unite is in mGy / MBq.S;

$$S(voxel_k \leftarrow voxel_h) = \sum_i \Delta_i \frac{\phi_i(voxel_k \leftarrow voxel_h)}{m_{voxel_k}}$$

Where, Δ_i is the mean energy of radiation type i emitted per nuclear transformation.

$\phi_i(voxel_k \leftarrow voxel_h)$ indicates that it is the fraction of the energy emitted by voxel source h that is absorbed in the target voxel k, and m_{voxel_k} is the mass of the target voxel k [17].

S-values affects by some factors such as the source and target geometry, the type of material defined for the source and the target, the type and energy of radiation, the distance between the source and the target, and the type of material contained therein. S-values presented in the tables for the tumor cannot be used since the shape of the tissue and the position and size of the tumor are not already known in the therapeutic or diagnostic applications. In this study, S values for NETs were also calculated.

III. Results

Table 2 shows S-values for 9 patients who underwent PET/CT examination 60 minutes after intravenous injection of ^{68}Ga-DOTATATE. These values are obtained during a voxelized source of ^{68}Ga was assumed to be a whole-body positronic source with actual distribution in different organs. The spleen (p1, p2, p4, p5, p6, and p8) and the bladder (p3, p7, and P9) followed by the kidney, the pituitary, the liver, and the lung have the highest S-values among different segmented organs of patients. The calculated mean of the S-values of each organ over all of the patients show that the spleen with 6.26E-05 ± 1.47E-05 (± one standard deviation) in the unite of mGy/MBq.S, has the largest value. After it, the bladder, the kidney, the liver, the pituitary, and the lung with values of 5.17E-05 ± 3.08E-05, 3.41E-05 ± 7.68E-06, 2.08E-05 ± 4.12E-06, 1.62E-05 ± 5.74E-06, and 8.47E-06 ± 2.47E-06 are the more pronounced organs, respectively. When the total body is considered a united target, S-values are in the order of several nGy/MBq.s with the 6.32E-06 as the highest value for P9 while the mean value is 4.87E-06 ±1.14E-06 mGy/MBq.S.

The acquired results show that tumors have S-values near or even more than the highest value

among other organs. The mean value over all of the 18 tumors of different patients is 4.68E-05 ± 3.68E-05, which is comparable to the spleens' mean value. Figure 3 depicts the S-values of various tumors based on their location inside the body. The S-value for tumor number 2 of the P3 (P3, T2) has the highest value (1.39E-04) located in the liver.

Figures 4 show the computed S-values for 3 patients (P3, P4, and P9). Five different organs for P3 and P4, and three organs for P9 are assumed as source organs. When source and target are the same organs, the highest S-value is acquired for that organ. For instance, the highest S-value is kept in the spleen itself when the spleen is a source. This behavior is repeated for all three patients with both of the sources. For a given target, the most crucial source of cross organ dose deposition can be found in these figures. For example, when the spleen is assumed as the target, the kidneys are the most essential source of cross organ dose.

A graphical approach to describing S-value distribution in a given volume is cumulative S-value-volume frequency distribution called S-value-volume histogram (SVVH) that, despite the lack of positional information, shows the order of uniformity of the S-value distribution in a given voxelized target. SSVH has a similar concept to dose-volume histogram (DVH) in radiation oncology [18]. Figure 5 shows SVVH of 11 segmented organs and all of the tumors of 9 patients.

Table 2. S- values (mGy/MBq.S) of different patients when total body PET scan is considered as the positron emission source. The whole-body scan (eye to tight) in some of the patients (P1, P3, P6, P7, and P8) resulted in the unavailability of necessary data for the segmentation of their skulls and brains.

Target	P1	P2	P3	P4	P5	P6	P7	P8	P9	Mean	SD
Spleen	5.71E-05	9.16E-05	3.82E-05	7.13E-05	4.54E-05	6.04E-05	6.41E-05	6.30E-05	7.23E-05	6.26E-05	1.47E-05
Lung	5.45E-06	1.00E-05	4.80E-06	6.32E-06	8.43E-06	7.90E-06	9.54E-06	1.23E-05	1.15E-05	8.47E-06	2.47E-06
Skull	-	2.50E-06	-	1.51E-06	1.22E-06	-	-	-	2.05E-06	1.82E-06	4.93E-07
Kidney	2.93E-05	4.92E-05	3.07E-05	4.06E-05	2.19E-05	2.74E-05	3.36E-05	3.98E-05	3.44E-05	3.41E-05	7.68E-06
Pituitary	1.23E-05	2.25E-05	1.24E-05	7.66E-06	1.07E-05	1.41E-05	1.91E-05	2.12E-05	2.55E-05	1.62E-05	5.74E-06
Liver	1.63E-05	2.00E-05	1.80E-05	1.85E-05	1.75E-05	2.40E-05	2.37E-05	1.92E-05	3.01E-05	2.08E-05	4.12E-06
Spine	4.76E-06	6.24E-06	3.87E-06	3.40E-06	4.34E-06	4.74E-06	5.17E-06	5.32E-06	6.26E-06	4.90E-06	9.17E-07
Heart	5.04E-06	6.51E-06	4.95E-06	4.66E-06	5.61E-06	5.23E-06	6.95E-06	6.88E-06	7.08E-06	5.88E-06	9.15E-07
Rib	2.98E-06	4.14E-06	2.35E-06	2.82E-06	3.07E-06	4.15E-06	4.11E-06	4.34E-06	5.12E-06	3.68E-06	8.50E-07
Brain	-	1.37E-06	-	8.86E-07	6.87E-07	-	-	-	1.02E-06	9.90E-07	2.49E-07
Tumor1	4.94E-05	-	1.14E-04	8.95E-05	2.82E-05	4.43E-06	-	-	-	4.68E-05 (All of the 18 tumors)	3.68E-05
Tumor2	4.35E-05	-	1.39E-04	7.88E-05	-	3.56E-05	-	-	-		
Tumor3	4.68E-05	-	3.56E-05	6.35E-06	-	2.18E-05	-	-	-		
Tumor4	2.40E-05	-	2.25E-05	7.14E-05	-	-	-	-	-		
Tumor5	-	-	-	2.53E-05	-	-	-	-	-		
Tumor6	-	-	-	6.34E-06	-	-	-	-	-		
Total Body	4.53E-06	6.70E-06	2.93E-06	4.04E-06	4.20E-06	4.23E-06	5.15E-06	5.72E-06	6.32E-06	4.87E-06	1.14E-06

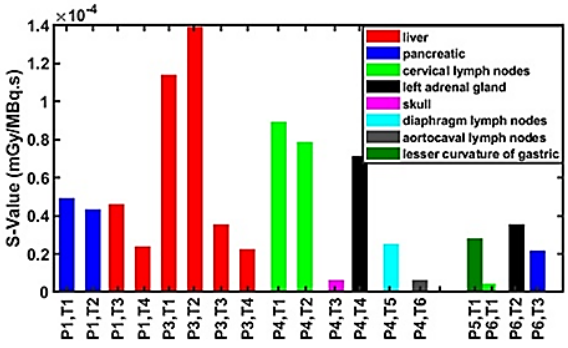

Figure 3. S-values of the tumors in different locations inside patients‘ organs when total body PET scan is considered as the positronic emission source.

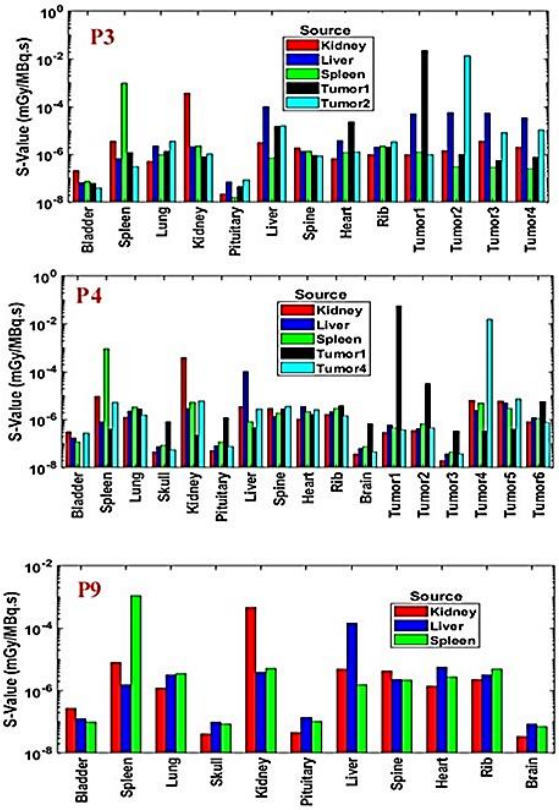

Figure 4. The S-values resulted from the distributed voxelized sources for three patients (p3, p4 and p9). To obtain these S-values, just one of the organs (kidney, liver, spleen or one of the tumors) were considered as a source in the separate simulations.

The results were calculated from the total body positronic voxelized source. For example, 100% of the volume of the spines of all patients received at least 2.0E-6 mGy/MBq.S.At the same time, the maximum values for various patients ranged between 7.0E-6 to 10E-6 mGy/MBq.S, which received in the minimum percent volume of a patient’s spine. A similar analysis could be done for other organs.

In this study, since the pictures were taken in a certain time and due to the lack of time-activity curve, the absorbed dose received to each patients’ organs cannot be calculated. But the initial dose rate was computed from the activity in the patient body at a specific period of time. The spatial dose rate distribution in the organs of P5 is shown in Figure 6. High dose values in these figures are obvious for the spleen, liver, kidneys, and bladder. The values of deposited doses in some parts of the spine and ribs nearest to the organ with a higher concentration of the ^{68}Ga are more considerable.

IV. Discussion

In this study, the S-values are calculated in different organs of 9 patients resulting from the distribution of the [^{68}Ga]DOTATATE as a new radiopharmaceutical tracer in the positron emission tomography to detect neuroendocrine cancerous tumors. We used PET/CT images as a voxelized source and geometry of the patient body in the Gate/Geant4 Monte Carlo code. The map of the deposited dose as the output of Gate was utilized to calculate S-values using MIRD formalism in the patients' organs.

To increase the speed of Monte Carlo simulations, we defined the positronic source that neglects gamma rays that are directly emitted from the ^{68}Ga and just consider positron liberated from the radionuclide and subsequent annihilation photons. This definition of source caused some approximation in the final results. Instead of the definition of spectra for different emitted positrons in the positronic source, they are assumed to be monoenergetic. This assumption leads to some errors in the dose distribution near the source due to variation in the positron particle ranges.

At the registration step, the pixel size of CT images changes to become as the PET through a combination and average on the Hounsfield unite (HU) of neighbor pixels in the CT images. Hence, the attenuation map of the patient’s body modifies to coarser pixel size. Whenever this will speed up

the run of the Monte Carlo code, some fluctuations in the absorbed dose will exist that are more severe for an organ with higher inhomogeneity between its original pixels. Another source of uncertainty that should be addressed in the segmentation step is the existence of air in some organs. Somewhere in the body, there are air cavities that should be defined in the input file of the Monte Carlo code as the air material. In this study, it is considered as the water leading to higher attenuation of gamma rays in their path to target organs. The body part below the bladder is cut away in the present study. The value of activity in the deleted organs is negligible, but this also can affect the cross-organ dose deposition in deficient order. The backscattering of gamma rays for the organs near these cropped organs can have a negligible effect on dose deposition.

While the determination of ^{68}Ga S-value has not been reported in the literature, some studies have been performed on the determination of [^{68}Ga]DOTATATE absorbed dose [14, 19, 20]. Walker et al. have measured the absorbed dose of different organs from PET/CT images using OLINDA/EXM software. The spleen, bladder, kidneys, and liver were recognized as the critical organ [20]. Bodei et al. have also reported a higher absorbed dose per injection activity in the spleen, bladder, kidneys, adrenals, and liver [19]. In this study, as shown in Figure 6, the spleen, liver, and kidneys have the maximum dose rate distribution in organs of the p5, which is consistent with other studies.

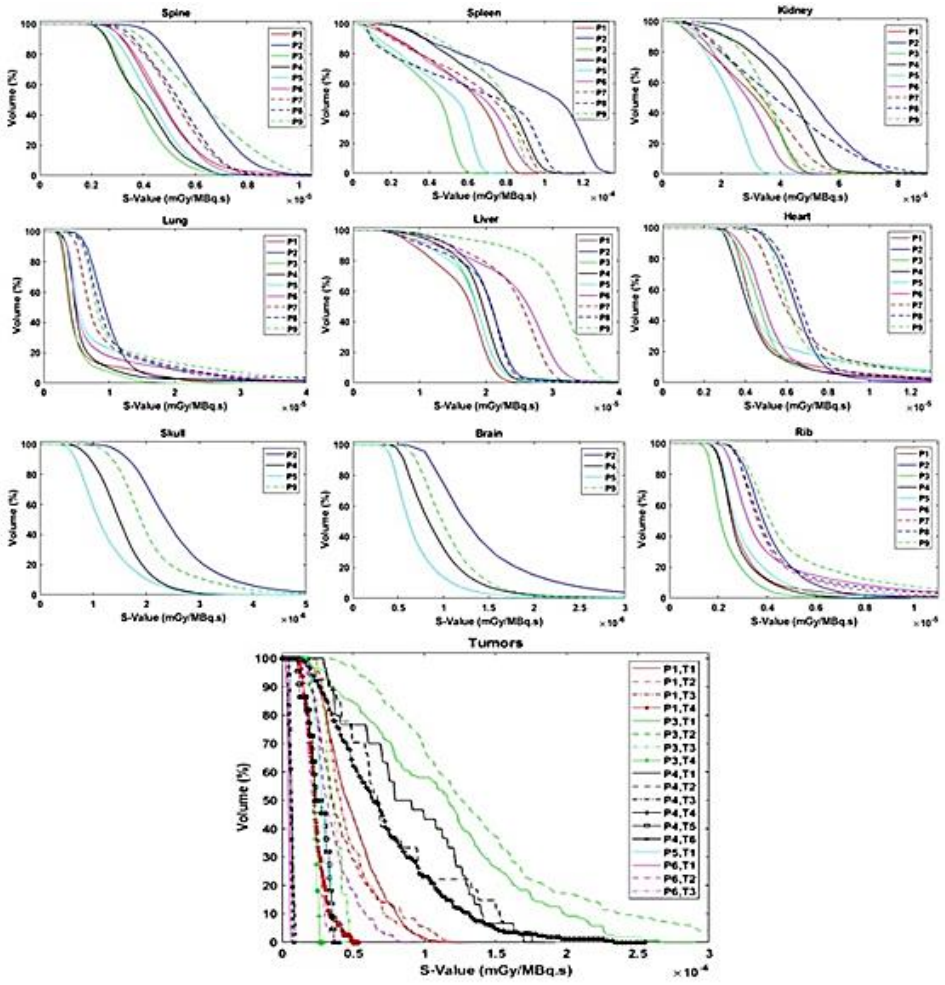

Figure 5. S-value volume histogram (SVVH) of the organs of 9 patients (p1 to p9) for ^{68}Ga-DOTATATE distribution inside body that extracted from PET scan. Total body was considered as a voxelized source. These results were calculated from the simulations assumed ^{68}Ga just as a distributed positron emission source (where direct gamma-rays from 68Ga were neglected and annihilation photons were considered).

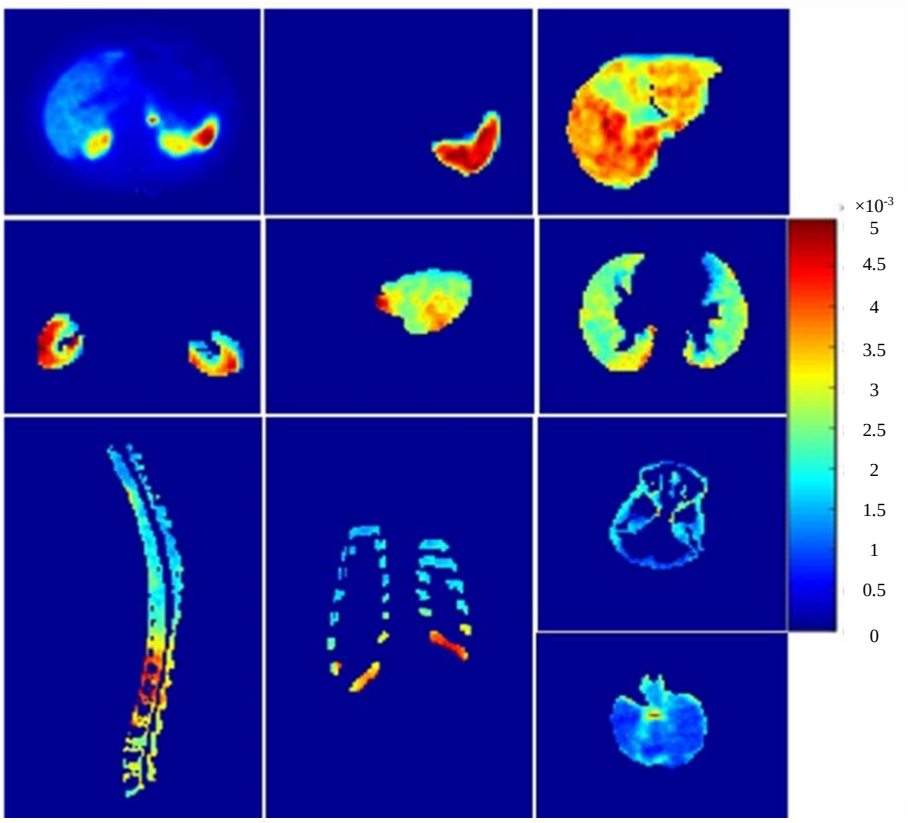

Figure 6. Dose rate distribution in organs of the p5. From up to down, and left to right: whole body, spleen, liver, kidneys, heart, lungs, spine, ribs, skull and brain. The unit of the common color bar between all figures is Gray (Gy).

The study carried out by Josefsson et al. aimed at compare the effect of different phantoms in S-value extraction for [^{68}Ga]DOTATATE, the absorbed dose was determined based on the CEP and the more recent ICRP 110 reference voxel phantoms. The highest values of absorbed dose coefficient are acquired in the spleen, pituitary, kidneys, adrenal glands, and liver, respectively [14]. This study showed that the effective dose is slightly overestimated using CEP compared to the ICRP 110 phantoms.

The results of Josefsoon et al. study indicated that phantom selected could affect the amount of absorbed dose. So, in this study, the S-values of ^{68}Ga was determined from PET/CT images. The obtained results show that the spleen has the highest mean S-value among all tissues, followed by the bladder, kidneys, liver, and pituitary. While the mean S-value for the spleen is higher, when we depended on factors such as the concentration of tracer agents in different organs the geometrical and structural aspects of the patient like weight, height, etc.

The results of this study was also compared with the dose factors extracted from OLINDA/EXM version 1.0 for an adult man [21]. The OLINDA/EXM code is the second-generation personal computer software for internal dose assessment in nuclear medicine. This code uses the same technical basis as the RADAR system and replaces the widely used MIRDOSE 3.1 code [22]. Whereas the main functions of MIRDOSE were retained in OLINDA/EXM code, some new phantoms and models were added.

Table 3 shows a comparison of the dose factors available in OLINDA/EXM version 1.0 and the P3 [19]. Some differences are obvious between these results. The most data adaption was observed for

the dose factor of the spleen: spleen and liver: liver. It should be mentioned that the dose factor presented in OLINDA/EXM is obtained for a specific phantom. At the same time, the physiological and anatomical characteristics are different from one person to another. The discrepancy between the results of this study with OLINDA/EXM can be related to the mentioned differences among the patients, leading to the distinct distribution of activity in each organ of the patients. The absorbed dose estimation of the radiopharmaceuticals needs to be calculated in the computational phantoms. These phantoms have been developed gradually to present much reasonable representation of the body. The Fisher–Snyder phantom is one of the earliest computational phantoms that utilizes different geometric shapes, including cylinders, spheres, and cones [23]. Also, the calculations are based on Monte Carlo simulations of radiation transport in these phantoms, which means the simulation of the particles and photons through the mentioned different structures with the density and atomic composition considered based on the literature. It should also be noted that in the case of a PET radioisotopes like ^{68}Ga, in the organ as the source and target organ simultaneously, the dose absorbed by the positron is higher than the dose absorbed by gamma radiation. The structures of the organs, including size, shape and also organ distances are so important that, for example, the absorbed dose of the kidneys for ^{18}FDG radiopharmaceutical can differ about six-fold for an adult phantom (6.03E-02) and a1-year-old phantom (1.18E-02). On the other hand, MIRD method assumes the activity distribution in source organs is uniform which may not happen precisely in real conditions [24,25]. In addition to all of the above mentioned, the body and function of different organs of each person are different from the other person.

Therefore, today special patient dosimetry is recommended, especially in cases that require treatment. This comparison proved that the specific dosimetry should be done individually for each patient.

V. Conclusion

In the present study, we used images of 9 patients who underwent [^{68}Ga]DOTATATE examination to calculate S-values in various organs using patient-specific dosimetry by Monte Carlo simulation. The highest S-values were observed in the spleen, bladder, kidneys, liver, and pituitary. Comparing the S-values extracted from OLINDA for an adult man and patient 3 showed apparent differences between these results. This comparison proved the importance of specific dosimetry in clinical trials.

Table 3. The comparison between S-values (mGy/MBq.S) which extracted from OLINDA for an adult male and the patient P3.

	Targets											
	Spleen		Kidney		liver		lung		Brain		Total body	
	OLINDA	P3	OLINDA	P3	OLINDA	P3	OLINDA	P3	OLINDA	P3	OLINDA	P3
Spleen	7.0E-4	7.3E-4	4.5E-6	2.4E-6	5.3E-7	6.8E-7	1.1E-6	7.9E-7	1.9E-8	-	2.5E-6	-
Kidney	4.5E-6	2.8E-6	4.3E-4	2.8E-4	2.0E-6	2.4E-6	4.9E-7	3.9E-7	4.8E-9	-	2.5E-6	-
Liver	5.3E-7	6.6E-7	2.0E-6	2.3E-6	7.5E-5	7.2E-5	1.3E-6	1.7E-6	1.7E-8	-	2.5E-6	-
Total Body	2.5E-6	3.8E-5	2.5E-6	3.1E-5	2.5E-6	1.8E-5	2.4E-6	4.8E-6	2.2E-6	2.2E-6	2.3E-6	2.9E-6

References

1. G. Fink, D.W. Pfaff, J.E. Levine, *Handbook of neuroendocrinology*, Academic Press (2012).
2. J.F. Tierney, C. Kosche, E. Schadde, et al., *68Gallium-DOTATATE positron emission tomography–computed tomography (PET CT) changes management in a majority of patients with neuroendocrine tumors*, Surg. (United States). 165, 178 (2019).
3. E.M. Wolin, *The expanding role of somatostatin analogs in the management of neuroendocrine tumors*, Gastrointest. Cancer Res. 5, 161 (2012).
4. M. Pavel, D. O'Toole, F. Costa, et al., *ENETS consensus guidelines update for the management of distant metastatic disease of intestinal, pancreatic, bronchial neuroendocrine neoplasms (NEN) and NEN of unknown primary site*, Neuroendocrinology. 103, 172 (2016).
5. W.A.P. Breeman, A.M. Verbruggen, *The 68Ge/68Ga generator has high potential, but when can we use 68Ga-labelled tracers in clinical routine?*, Eur. J. Nucl. Med. Mol. Imaging. 34, 978 (2007).
6. H.R. Maecke, M. Hofmann, U. Haberkorn, (68)*Ga-labeled peptides in tumor imaging.*, J. Nucl. Med. 46, 172 (2005).
7. A.R. Jalilian, *An overview on Ga-68 radiopharmaceuticals for positron emission tomography applications*, Iran. J. Nucl. Med. 24, 1 (2016).
8. S. Zolghadri, A. Jalilian, H. Yousefnia, *Absorbed dose assessment of 177 Lu-zoledronate and 177 Lu-EDTMP for human based on biodistribution data in rats*, J. Med. Phys. 40, 102 (2015).
9. I. Virgolini, V. Ambrosini, J.B. Bomanji, et al., *Procedure guidelines for PET/CT tumour imaging with 68Ga-DOTA- conjugated peptides: 68Ga-DOTA-TOC, 68Ga-DOTA-NOC, 68Ga-DOTA-TATE*, Eur. J. Nucl. Med. Mol. Imaging. 37, 2004 (2010).
10. M. Sandstrom, I. Velikyan, U. Garske-Roman, et al., *Comparative Biodistribution and Radiation Dosimetry of 68Ga-DOTATOC and 68Ga-DOTATATE in Patients with Neuroendocrine Tumors*, J. Nucl. Med. 54, 1755 (2013).
11. T.D. Poeppel, I. Binse, S. Petersenn, et al., *68Ga-DOTATOC Versus 68Ga-DOTATATE PET/CT in Functional Imaging of Neuroendocrine Tumors*, J. Nucl. Med. 52, 1864 (2011).
12. M. Fallahpoor, M. Abbasi, F. Kalantari, et al., *Practical nuclear medicine and utility of phantoms for internal dosimetry: Xcat compared with zubal*, Radiat. Prot. Dosimetry. 174, 191 (2017).
13. B. Quinn, Z. Dauer, N. Pandit-Taskar, et al., *Radiation dosimetry of 18F-FDG PET/CT: Incorporating exam-specific parameters in dose estimates*, BMC Med. Imaging. 16, 1 (2016).
14. A. Josefsson, R.F. Hobbs, S. Ranka, et al., *Comparative Dosimetry for 68 Ga-DOTATATE: Impact of Using Updated ICRP Phantoms, S Values, and Tissue-Weighting Factors*, J. Nucl. Med. 59, 1281 (2018).
15. D. Scheme, N. Data, E.C. Transitions, *Table of radionuclides - 68Ga*, PP. 1–7 (2012).
16. M. Ljungberg, K. Gleisner, *Hybrid Imaging for Patient-Specific Dosimetry in Radionuclide Therapy*, Diagnostics. 5, 296 (2015).
17. W.E. Bolch, L.G. Bouchet, J.S. Robertson, *MIRD pamphlet No. 17: the dosimetry of nonuniform activity distributions--radionuclide S values at the voxel level. Medical Internal Radiation Dose Committee.*, J. Nucl. Med. 40, 11S (1999).
18. R.E. Drzymala, R. Mohan, L. Brewster, *Dose-volume histograms.*, Int. J. Radiat. Oncol. Biol. Phys. 21, 71 (1991).
19. L. Bodei, V. Ambrosini, K. Herrmann, *I. Modlin, Current Concepts in 68 Ga-DOTATATE Imaging of Neuroendocrine Neoplasms: Interpretation, Biodistribution, Dosimetry, and Molecular Strategies* , J. Nucl. Med. 58, 1718 (2017).
20. R.C. Walker, G.T. Smith, E. Liu, et al., *Measured Human Dosimetry of 68Ga-DOTATATE*, J. Nucl. Med. 54, 855 (2013).
21. M.G. Stabin, R.B. Sparks, E. Crowe, *OLINDA/EXM: The Second-Generation Personal Computer Software for Internal Dose Assessment in Nuclear Medicine.*, J Nucl Med. 46, 1023 (2005).
22. M. Stabin, J Siegel, J. Hunt, et al., *The radiation dose assessment resource—an online source of dose information for nuclear medicine and occupational radiation safety [abstract]*. J Nucl Med. 42, 243 (2002).
23. W. Snyder, M. Ford, G. Warner, et al. *Estimates of absorbed fractions for monoenergetic photon sources uniformly distributed in various organs of a heterogeneous phantom.* J Nucl Med. 5, suppl 3 (1969).
24. M.G. Stabin, R.B. Sparks, E. Crowe. *OLINDA/EXM: The Second-Generation Personal Computer Software for Internal Dose Assessment in Nuclear Medicine.*J Nucl Med. 46, 6 (2005).
25. M.G. Stabin, J.A. Siegel. *RADAR Dose Estimate Report: A Compendium of Radiopharmaceutical Dose Estimates Based on OLINDA/EXM Version 2.0.* J Nucl Med. 59, 154–160 (2018).

How to cite this article

S. Karimkhani, H. Yousefnia, R. Faghihi, P. Gramifar, M. R. Parishan, Calculation of Gallium-68 Dose Factors for [68Ga] DOTATATE injected Patients: A Comparison with OLINDA database*, Journal of Nuclear Science and Applications*, Vol. **2,** No. **2, (2022),** P **30-40,**
Url: https://jonra.nstri.ir/article_1469.html, **DOI**: 1024200/jon.2022.1018